Turbulent Boundary Layer Perturbed by a Screen

R.D. Mehta*
Imperial College, London, England, UK

A detailed experimental investigation has been carried out on the effects of different types of screens on turbulent flow, in particular turbulent boundary layers. The boundary-layer turbulence is reorganized and the thickness reduced, thus making it less susceptible to separation. The aerodynamic properties of plastic screens are found to differ significantly from those of the conventional metal screens. The "overshoot" in mean velocity profile near the boundary-layer edge is shown to be a result of the effect of screen inclination on pressure drop coefficient. A more accurate formulation for the deflection coefficient of a screen is also proposed.

Nomenclature

C_f = skin-friction coefficient
d = screen wire diameter
F = force coefficient parallel to the screen surface
K = screen pressure drop coefficient, $\Delta p/q$
k = wave number
l = screen mesh length
P = total pressure
p = static pressure
Δp = static pressure drop across the screen
q = dynamic pressure, $\frac{1}{2}\rho U_e^2$
Re = Reynolds number, Ud/ν
Re_β = modified screen Reynolds number, $Ud/\beta\nu$
Re_θ = Reynolds number based on boundary-layer momentum thickness, $U\theta/\nu$
R_{uv} = shear correlation coefficient, $\overline{uv}/\sqrt{\overline{u^2}}\sqrt{\overline{v^2}}$
U, V, W = mean velocity components in the x, y, and z directions, respectively
U_e = local freestream velocity
U_{ref} = undisturbed freestream velocity at the screen position
u, v, w = fluctuating velocity components
x, y, z = streamwise, normal, and spanwise directions, respectively
α = screen deflection coefficient, ϕ/θ
β = screen open-area ratio $(1-d/l)^2$
δ_0 = undisturbed boundary-layer thickness at the screen position
θ = angle between incident flow and local normal to the screen or boundary-layer momentum thickness
ν = kinematic viscosity
ρ = density
ϕ = angle between emerging flow and local normal to the screen or power spectral density
ψ = stream function

Subscripts
0 = working section (undisturbed)
1 = upstream of screen
2 = downstream of screen
θ = screen inclined to incident flow

Presented as Paper 84-0538 at the AIAA 22nd Aerospace Sciences Meeting, Reno, Nev., Jan. 9-12, 1984; received March 28, 1984; revision received Oct. 1, 1984.

*Department of Aeronautics; presently with Department of Aeronautics and Astronautics, JIAA, Stanford University, Stanford, Calif. Member AIAA.

Introduction

SCREENS have been used to improve flow quality in wind tunnels since the 1930's. They are normally installed in the settling chamber to improve the mean flow uniformity and to reduce the intensity of the oncoming turbulence. This effect of screens has been studied widely over the years.[1-4] A review of the earlier works and thoughts on flow through screens is given by Corrsin.[5] Recent work has concentrated on using some of those ideas, for example, the manipulation of the existing turbulence so that the spectral transfer of the wave-number energy may be accelerated.[6-8] Another recent application of screens is to control or suppress boundary-layer separation, especially in wide-angle diffusers.

The first-order effect of a screen is to impose a static pressure drop proportional to the square of the flow velocity and to refract the incident (inclined) flow toward the local normal to the screen. These effects are described in terms of two parameters, the pressure drop coefficient K and the deflection coefficient α. We expect the functional relationships for K and α to be

$$K = f_1(\beta, Re, \theta) \tag{1}$$

$$\alpha = f_2(\beta, K, \theta) \tag{2}$$

Although the screen pressure drop coefficient is defined as the ratio of the static pressure drop across it (Δp) to the dynamic head of the approaching flow ($\frac{1}{2}\rho U_e^2$), in finite ducts, measuring Δp as a difference in static pressures across the screen leads to errors. By measuring $p_1 - p_2$ in a finite tunnel, one measures the actual pressure drop across the screen minus the drop in dynamic pressure across the screen due to boundary-layer displacement effects. So for all measurements in finite ducts, the pressure drop must be measured as a difference in total pressures. Although several expressions have been derived over the years for the pressure drop coefficient of a screen,[10-13] many of them were based on data from low β screens ($\beta < 0.5$) and were often contaminated by errors of the type discussed above. Although there is no wholly satisfactory formulation for predicting K, the one due to Wieghardt,[12]

$$K = 6.5\left[\frac{1-\beta}{\beta^2}\right]\left[\frac{Ud}{\beta\nu}\right]^{-0.33} \tag{3}$$

was found to be the most accurate in predicting the right trend over the velocity range $0 < U < 20$ m/s.[14,15]

The pressure drop coefficient of a screen, based on the magnitude of the flow velocity, is found to decrease with increasing flow inclination. Although several theoretical and semiempirical relations have been proposed for K_θ,[16-20] based mainly on a $\cos^2\theta$ relation, no universality has been noted.

Several workers[3,16,17,19,20] have also developed expressions for the deflection coefficient, but no satisfactory agreement has evolved for K_θ. This is partly due to difficulties in measuring the flow angles accurately and consistently. In fact, many of the earlier measurements of all the quantities suffered from poor or inadequate measurement techniques. A more detailed review of the earlier measurements is given in Ref. 15, whereas a more general review on flow through screens can be found in Ref. 21.

The objective of the present investigation was to study the flow of turbulent boundary layers through screens of different materials and open-area ratios, with emphasis on both the mean and turbulence quantities. Details of the perturbation produced by the screen, as well as the recovery from it, were studied. The effects of a screen on incident inclined flow, such as that found in wide-angle diffusers, were also established.

A more detailed account of the present investigation is given in Ref. 14, and full details of the experimental techniques and results can be found in Ref. 15. Results from this investigation have also been used to derive design rules for small, low-speed wind tunnels.[22,23]

Experimental Techniques

A 450×450-mm (18×18-in.) open-circuit blower wind tunnel was used for the measurements (Fig. 1). The tunnel incorporates a wide-angle diffuser and a filleted contraction with an area ratio of 7:1. The boundary-layer measurements were made in the main working section of constant cross-sectional area. For the inclined flow measurements, a rig was designed that could be attached to the downstream end of the working section. The arrangement consisted of a hinged wooden frame to which the screen was tacked. Wooden wedges inserted in the sides between the frame and the end of the working section and a false roof with a fairing ensured a uniform inlet flow to the inclined screen.

The boundary layer was tripped at the contraction exit by a 1-mm-diameter round wire (Fig. 1). The nominal tunnel speed for most of the measurements was 18 m/s. At this operating speed, the measured turbulence intensity level was 0.28%. Standard pitot tubes were used for the total pressure measurements, and the inclination and total pressure of the flow

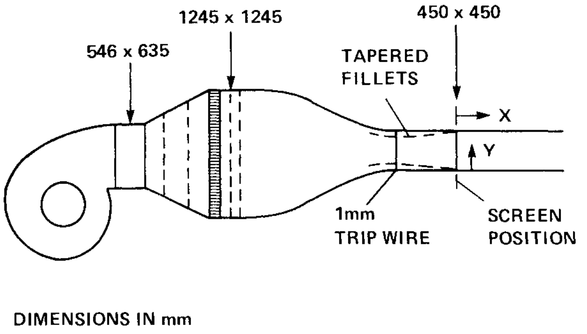

Fig. 1 Schematic of experimental rig.

Table 1 Details of screen samples

Screen	Wire diameter d, mm	Mesh length l, mm	Open-area ratio β
Steel	0.417	1.69, 1.59	0.556
Brass	0.274	1.27	0.614
Plastic coarse	0.289	1.21	0.578
Plastic fine	0.152	0.635	0.578
Steel (1)	0.376	1.69, 1.59	0.594

emerging from an inclined screen were measured using a three-hole yawmeter. All the turbulence measurements were made with conventional single and cross hot-wire probes using analog signal processing electronics. The wires were Wollaston elements with a 5-μm diameter and 1-mm long "active" platinum core. For the cross hot-wires, the spacing between the wires was also about 1 mm. For the spectrum measurements, hot-wire signals were recorded on an analog tape recorder and analyzed off-line on a Bruel and Kjaer spectrometer.

The measured geometric details of the screens and descriptive names used in this investigation are given in Table 1.

Results and Discussion

Mean Velocities and Skin-Friction Coefficient

The mean velocity profiles measured downstream of two screens are shown in Figs. 2a and 2b. The undisturbed boundary-layer profile shown in these figures was that measured at $x = 140$ mm, without the test screen in place. A fully developed turbulent boundary layer with an Re_θ of 1690 was obtained at the test flow speed of 18 m/s. A reduction in boundary-layer thickness is apparent, although the actual edge of the boundary layer is not clearly defined. The nonuniformities (or rippling) in the potential core, which seem to persist up to $x = 597$ mm for the steel screen, are presumably longitudinal vortices formed by the random coalescing of jets emerging from the screen pores. According to Bradshaw,[24] the rippling is more prominent for screens with $\beta < 0.57$. The steel screen has a β of 0.56. The velocity profile at $x = 597$ mm for the plastic coarse screen is extremely uniform away from the boundary layer. There are signs of an overshoot in the velocity profiles near the boundary-layer edge, particularly for the plastic coarse screen. The behavior of the two plastic screens was similar, except that the plastic fine screen produced a bigger overshoot.

The main differences in the mean flow between the plastic and metal screens relate to the overshoot, discussed below, and the rippling in the core flow. Several researchers[24-26] have found that screens with open-area ratios of less than about 0.5-0.6 produce a flow that is unstable with both spatial and temporal variation. The cause of instability is explained[24] as the random coalition of jets emerging from the screen pores. An investigation of the weaving properties revealed that the plastic strands were necked at the nodal points so that they were embedded within each other. This implies that fibers cannot slide over each other and hence the original uniform weave is maintained. This also means that the overall thickness of the plastic screens is less, thus making them more coplanar. It seems feasible that the chances of the flow remaining straight and parallel as it goes through the pores would improve if the screen was nearly coplanar. The overall measured thickness of the steel screen was $2.2d$ whereas that of the plastic coarse screen, which produced the most uniform core flow, was $1.8d$.

The skin-friction distribution (Fig. 3) shows the expected increase downstream of all the screens and then a monotonic decreasing recovery at different rates. Although some of the increase in C_f is due to boundary-layer displacement effects, C_f being normalized by the local U_e, the actual wall shear stress must also be expected to increase since the mean velocity gradient near the wall increases (Fig. 2). The skin-friction values at the last measurement location ($x \sim 600$ mm) are still higher for all screens than the extrapolated "without screen" value. The plastic fine screen produces the maximum perturbation; this may seem surprising since it does not correlate with β, which is lowest for the steel screen (0.56) and highest for the brass screen (0.61). This is due to the fact that, for a given β and Re, a plastic screen was found to impose a higher pressure drop than a metal screen.[15] Note that a screen imposes the static pressure drop in a streamwise distance

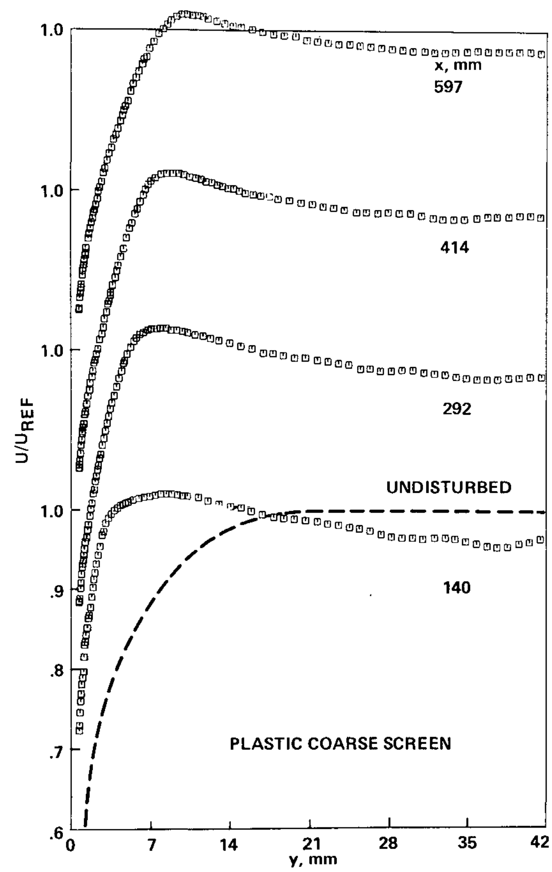

Fig. 2a Mean velocity profiles downstream of the steel screen.

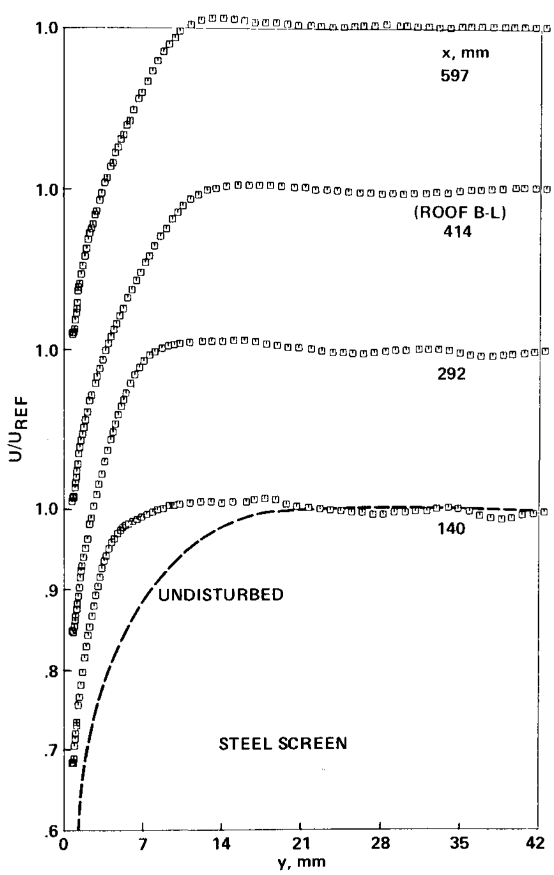

Fig. 2b Mean velocity profiles downstream of the plastic coarse screen.

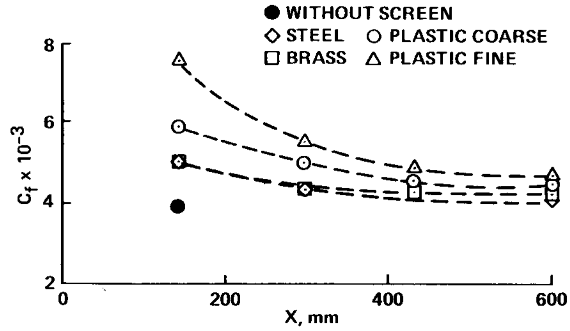

Fig. 3 Streamwise distribution of skin-friction coefficient.

equivalent to about one δ_0 and the local behavior of the C_f distribution is similar to that expected in a boundary layer subjected to a sudden favorable pressure gradient.

Turbulence Quantities

Extensive measurements of the Reynolds stress components ($\overline{u^2}$, $\overline{v^2}$, and $\overline{uv}$) were made downstream of four screens (two metal and two plastic). Since the effects of all four screens were qualitatively similar, the results for only one screen (plastic coarse) are presented here. As seen in Figs. 4a-c, the action of the screen is to reduce drastically all the stresses in the boundary layer and to add some turbulence in the core flow. Almost full recovery of the boundary-layer turbulence is obtained by the last measurement station ($x = 562$ mm). Once again, the reduction in the Reynolds stresses could be explained in terms of the sudden favorable pressure gradient effects. However, the screen also has other, first-order, effects on the turbulence.

The attenuation in $\overline{u^2}$ is associated with the fact that a local velocity excess meets greater resistance at the screen. The reduction in $\overline{v^2}$ is associated with the action of a screen in refracting the oncoming flow toward the local normal. The qualitative trends of the reduction factors for these stresses in the boundary layer are in agreement with the theoretical results due to Taylor and Batchelor,[3] which ignored inertia and viscous forces. The implication, therefore, is that viscosity does not play a significant role in the turbulence-reduction process.

There are also two sources of turbulence. If the local Re_β of the screen wires is greater than about 80 (true for most practical applications), the wire wakes will be turbulent and the screen will contribute turbulence to the flow. This addition is clearly seen in the core region of the $\overline{u^2}$ and $\overline{v^2}$ profiles (Figs. 4a and b). Another source of turbulence is through the nonuniformities in mean velocity produced by the screen in the core flow (Figs. 2a and 2b), which are then acted upon by Reynolds stresses. For example, the slight rippling in the $\overline{uv}$ profile at $x = 105$ mm (Fig. 4c) comes from the dominant production term in the $\overline{uv}$ transport equation, $\overline{v^2}(\partial U/\partial y)$ (see Ref. 15). It is evident from the results presented in Figs. 4a-c that, for the present inlet conditions in the core flow, this additional turbulence persists for at least about 200 screen mesh lengths. The structure and scale of the oncoming turbulence also seem to be affected by the screen.

The shear correlation coefficient R_{uv} results (Fig. 4d) show that, in the region of recovery from the effects of the perturbation, the efficiency of maintenance of shear stress is reduced. The reduction is not as marked as the shear stress itself since the intensities are also reduced, but the structural changes involved are obviously large. Recovery was found to be much faster in the region nearer the wall (but still in the outer layer) as indicated by the profile at $x = 257$ mm. Again, the maximum R_{uv} in the boundary layer was found to recover to the undisturbed value by $x = 562$ mm for all the screens.

The spectra results for ϕ_{11} at $y = 0.25\delta_0$ are shown in Fig. 5. The spectral density is normalized by U_{ref} so that direct comparison is more justifiable. The area under the curve is thus equal to the normalized turbulence intensity. The $-5/3$ law, which comes from Kolmogorov's universal equilibrium assumptions, is also plotted for the undisturbed case to verify the normality of the measured spectra. The spectral density in the low wave-number (energy-containing) range is reduced by the screen. At higher wave numbers, the spectrum now falls off more slowly, indicating a contribution from the screen wire wakes. The spectrum starts to recover at $x = 257$ mm. The reduction at low wave numbers seems to imply that the screen reduces the scale of the oncoming turbulence. However, it is also suggested[5-9] that by adding a suitable high wave number, the spectral transfer of the pre-existing low wave-number energy may be accelerated, thus increasing its decay rate.

Overshoot in Mean Velocity Profiles

In the results presented above, the most interesting phenomenon observed has been the overshoot in the mean velocity profile near the boundary-layer edge. In effect, we get a velocity or total pressure excess where there was a defect, i.e., in the boundary layer. Of course, this overshoot may be beneficial in terms of tackling a given pressure gradient in a wide-angle diffuser.

Other workers[27-29] have also noted this overshoot, mainly for screens with $K > 1$. However, none of them gave a satisfactory explanation for the effect (see Ref. 15 for details). The same erroneous explanations were also quoted by Laws and Livesey in their review article.[21]

For the overshoot to occur, the streamlines near the boundary-layer edge have to undergo a pressure drop that is less than the drop along the center streamline and also less than that along streamlines within the boundary layer. In a finite tunnel, the streamlines passing through the screen very

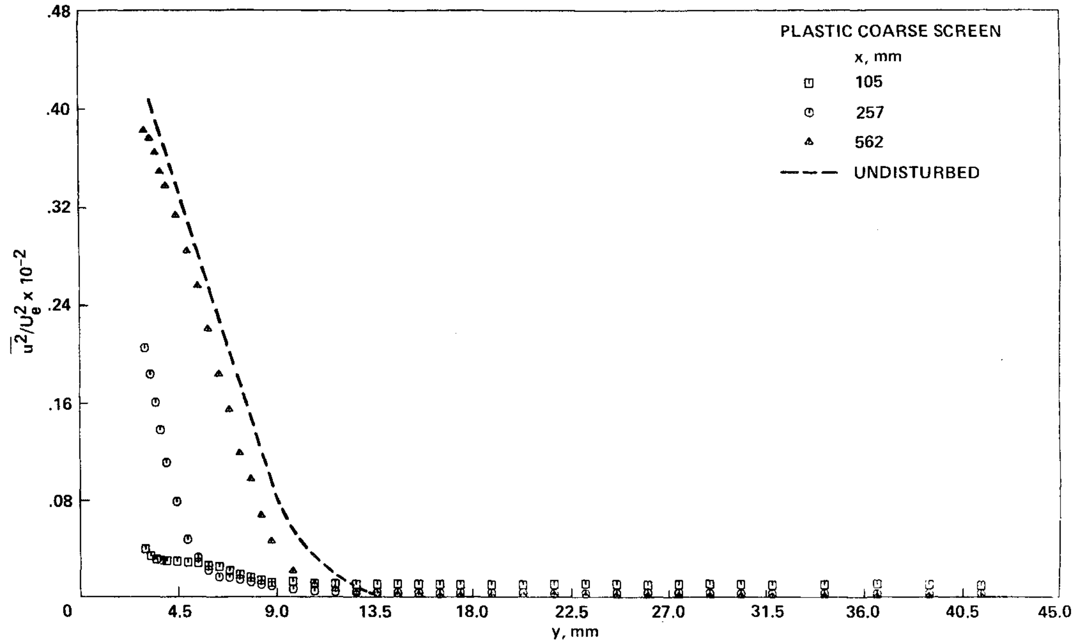

Fig. 4a $\overline{u^2}$ profiles downstream of the plastic coarse screen.

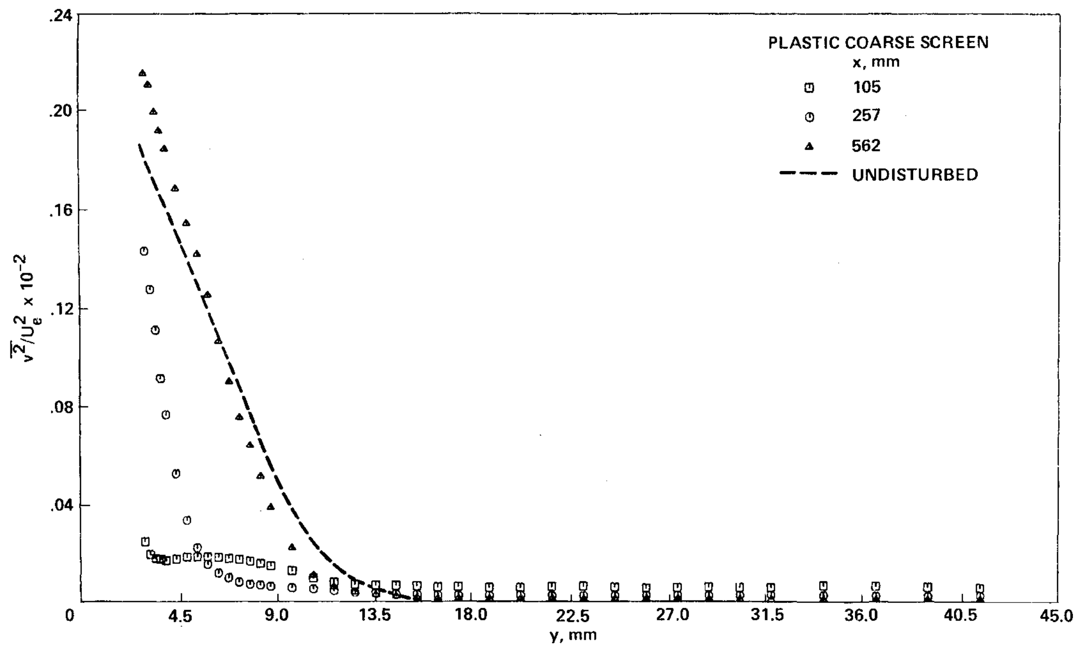

Fig. 4b $\overline{v^2}$ profiles downstream of the plastic coarse screen.

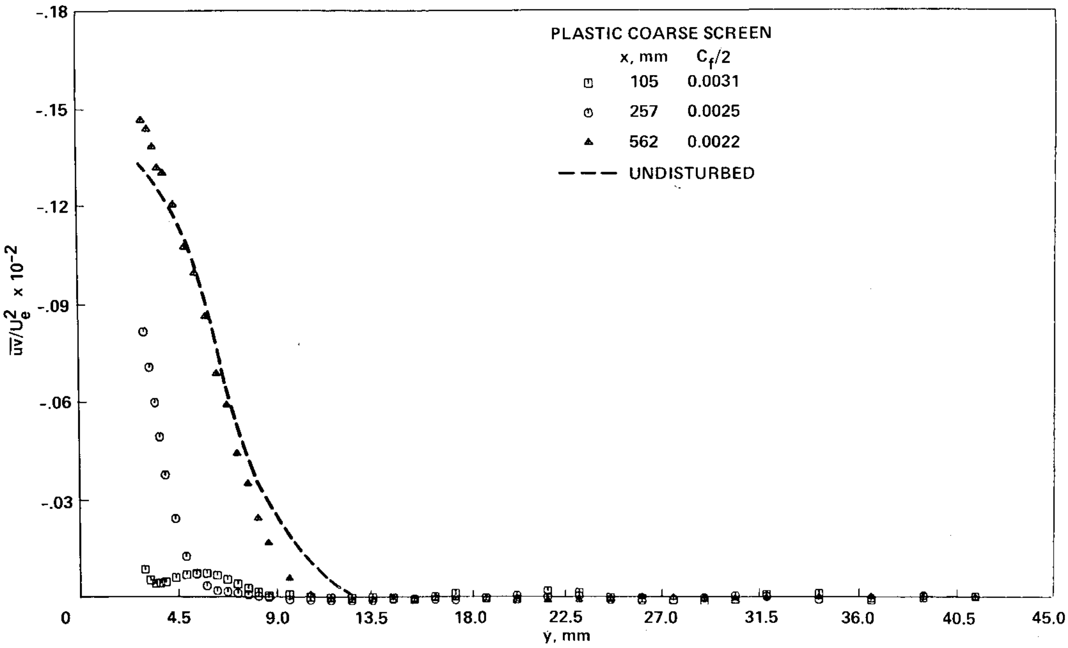

Fig. 4c $\overline{uv}$ profiles downstream of the plastic coarse screen.

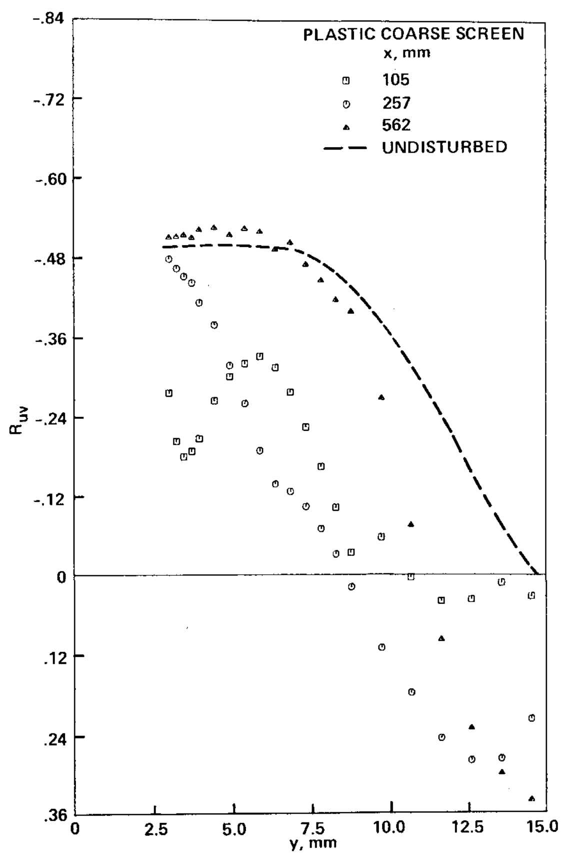

Fig. 4d R_{uv} profiles downstream of the plastic coarse screen.

close to the wall and those on the tunnel centerline must be expected to be straight and parallel. Now, since the boundary layer is thinned down by the screen, there must be a region, presumably near the boundary-layer edge, where the streamline inclination is at a maximum.

Now, as mentioned above in the introduction and confirmed below, K is found to decrease with increasing flow inclination following the relation:

$$\Delta P = K \times \tfrac{1}{2}\rho U^2 \times \cos^m\theta \tag{4}$$

ΔP will be a minimum where $U^2\cos^m\theta$ is a minimum, presumably somewhere near the boundary-layer edge, which could result in the overshoot. Although K is also a function of Re (and hence U), the dependence is weak near the boundary layer edge, where $U \sim 18$ m/s.[14] Anyway, K increases with decreasing Re, so this effect cannot be responsible for the overshoot.

In order to verify that the point of minimum pressure drop is at a finite distance from the wall, the pressure drop along individual streamlines was calculated from the velocity profiles. Figure 6 shows the pressure-loss deficit along a streamline plotted against the stream function ψ. The curves for all the screens have a well-defined point of minimum pressure drop at a finite distance from the wall. The results indicate that at a given streamwise station, the overshoot for the steel screen should be farther away from the wall than that for the plastic coarse screen. This is indeed the case, as seen in Figs. 2a and 2b. The results also indicate that the plastic screens should produce a bigger overshoot than the metal screens since they produce a bigger deficit in pressure loss. This was also in general agreement with the extent of the overshoot in the velocity profiles. Note that the pressure deficit will approach zero only at infinity. At intermediate values, the deficit will be equal to

$$K-(p_l-p_2)/\tfrac{1}{2}\rho U_e^2 \tag{5}$$

Of course, the same effect should also be obtained if the screen were inclined (instead of the streamlines). This was verified by measuring the total-pressure profiles downstream of the steel screen with the screen straight (in side view) and the screen deliberately curved into a semicircular shape (Fig. 7). The inclined part of the screen produced a distinct overshoot ($\sim 20\%$) near the boundary-layer edge. The profiles collapse well for the region of zero inclination before diverging again as the inclination effects due to the upper half of the screen curvature start to dominate in the same way.

In practice, screens installed in wind tunnels will always deflect somewhat due to wind loading. On measuring the streamwise deflection of the screens on the tunnel centerline,[15] it was found that the plastic screens deflected about 60% more (at $U = 18$ m/s) than the metal screens. Now since the deflection and the overshoot for the plastic screens were found to be speed-dependent,[14] this suggests that the overshoot for these screens was more a result of screen inclination.

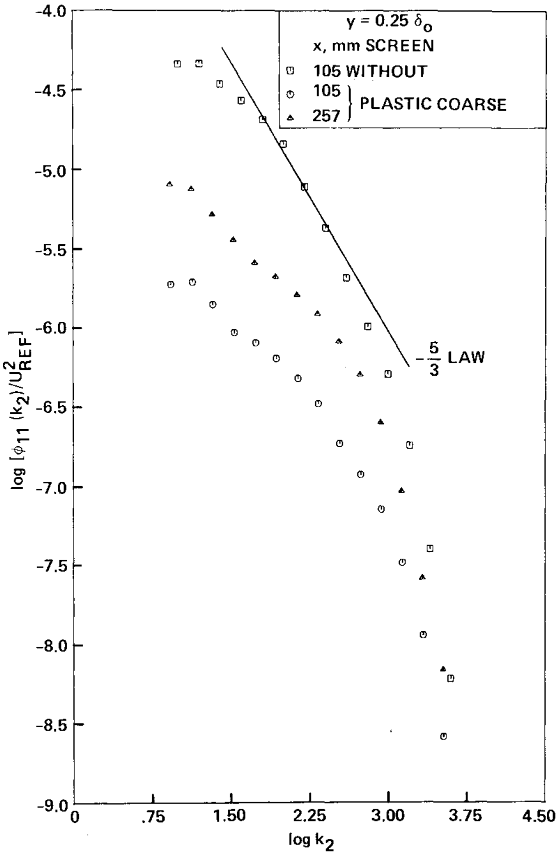

Fig. 5 ϕ_{11} spectra at $y = 0.25\delta_0$.

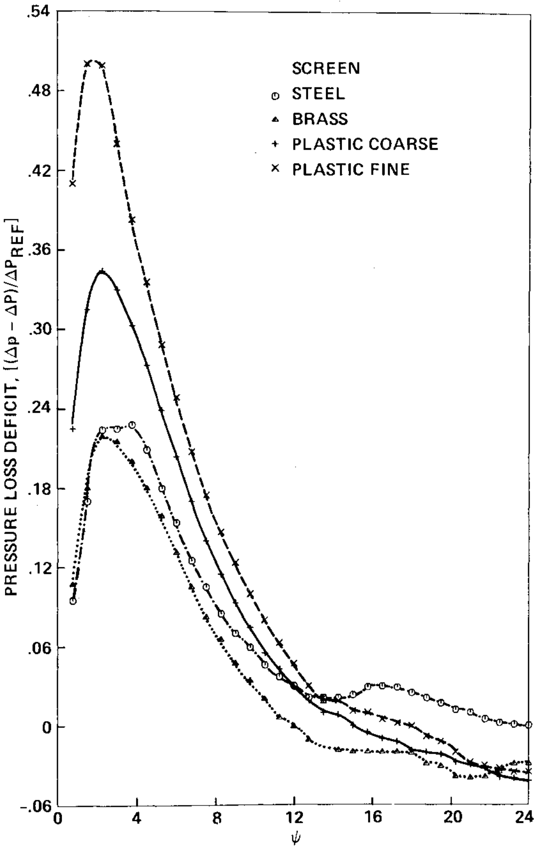

Fig. 6 Pressure-loss deficit along streamlines.

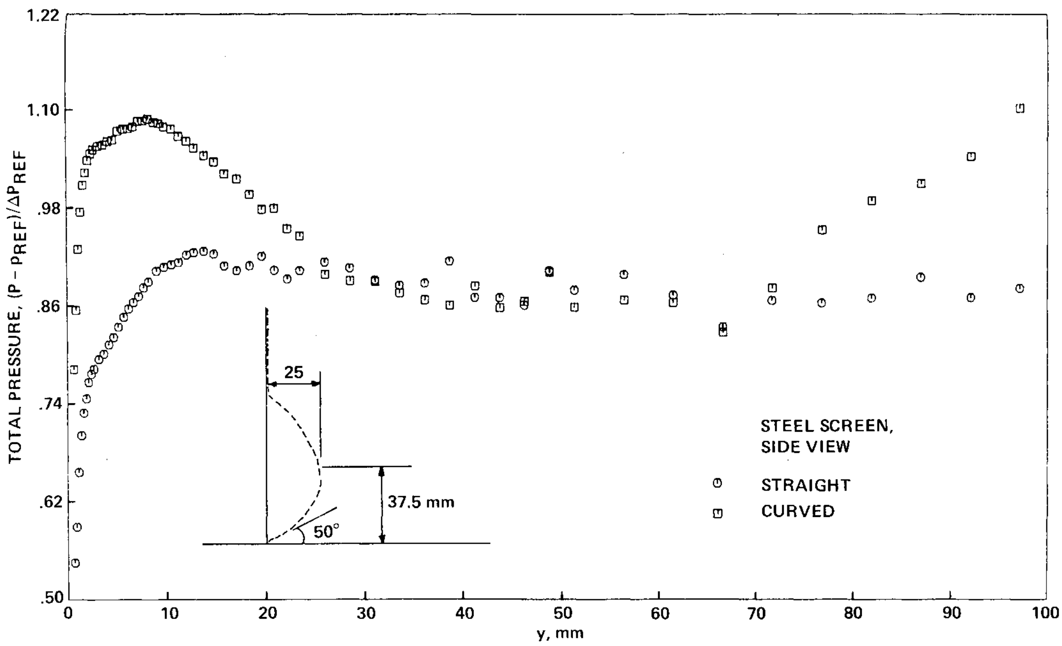

Fig. 7 Effect of screen curvature on total pressure profile at $x = 50$ mm.

The overshoot observed by Owen and Zienkiewicz[27] with their solid grid must have been due to streamline inclination. The reason this effect is observed mainly for screens with $K > 1$ is that as K increases, the boundary layer is thinned down more and so the streamline inclination is increased. So, as regards the overshoot, the important parameters are the pressure drop coefficient for a rigid screen, which determines the streamline inclination, and the flexibility of the screen, which determines the screen inclination.

Inclined Screen Results

It is evident from the results discussed above that streamline or screen inclination plays an important role in determining the details of the emerging flowfield. Since the flow in a wide-angle diffuser will be inclined to a normal screen, an investigation of flow through inclined screens was conducted.

The results for the variation of pressure drop coefficient K_θ, with screen inclination θ, for the steel (1) screen is shown in Fig. 8. Also shown in this figure is a $\cos^m\theta$ relation (with m as

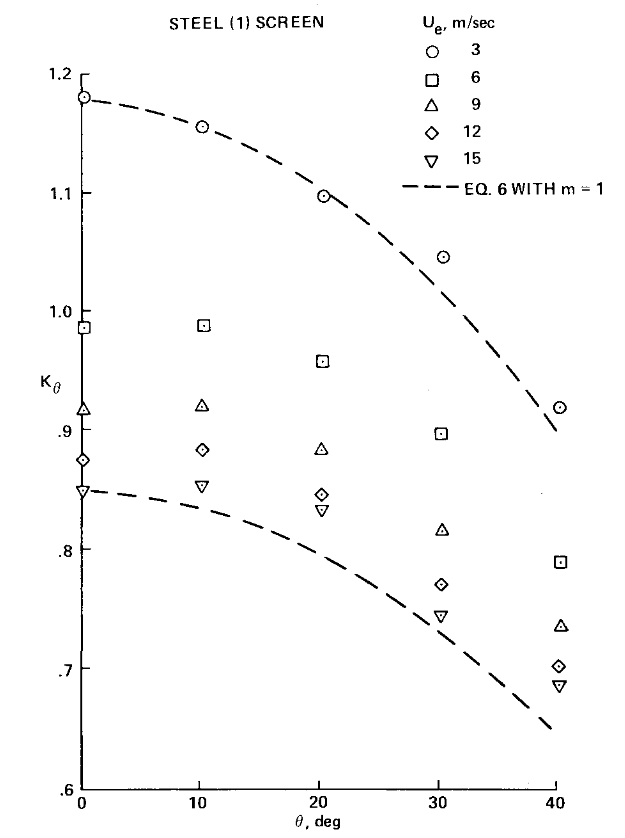

Fig. 8 K_θ vs θ for the steel (1) screen.

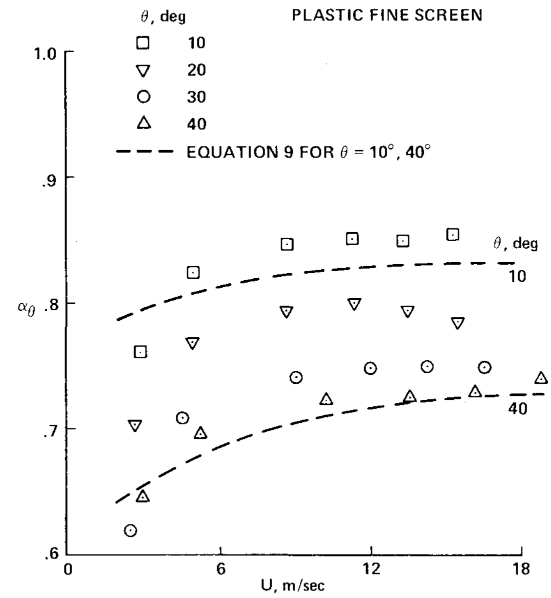

Fig. 9 Variation of α_θ with flow speed for the plastic fine screen.

an empirical constant), forced to fit K (at $\theta = 0$) at the two velocity limits. Results for all of the screen samples listed in Table 1 showed that, for screens with $\beta \sim 0.6$, a $\cos\theta$ relation ($m = 1$) agrees to within 7%.[14,15] However, for screens of lower β (~ 0.3), $m = 1.4$ gave a better fit.[14] The implications of this seem feasible since one would expect a screen with low β (wires closer together) to be affected more by inclination than one with a higher β (wires further apart). Ignoring the complex interaction of the interwoven wire wakes, an intuitive "normal component of velocity" argument of course suggests a $\cos^2\theta$ relation, as proposed by some of the early researchers.[16] However, the relation proposed here also agreed very well (see Ref. 15) with some previous data.[2,20] So the proposed semiempirical relation for K_θ is

$$K_\theta = K \cos^m\theta \tag{6}$$

with $m \sim 1.0$ for screens with $\beta \sim 0.6$, and $m \sim 1.4$ for screens of lower β (~ 0.3).

The deflection coefficient α_θ ($= \phi/\theta$) is plotted for the plastic fine screen in Fig. 9. As expected, for a given θ, at the higher speeds where Re is the highest, the value of α_θ approaches an asymptote. However, there is also a strong dependence of α_θ on θ, with α_θ decreasing with increasing θ. Most of the early workers[13,16] did not appreciate this dependence, which was again stronger for the plastic screens. It is proposed[14,15] that the sign of $d\alpha_\theta/d\theta$ is at least partly related to the screen β, or more strictly to the screen K.

In the present investigation, semiempirical relations for α and α_θ were derived using the present data only. The main difference between the present approach and previous attempts was in realizing that F_θ/θ cannot be correlated with K_θ for all θ. There is a strong dependence of this function on θ which must be modeled. The suggested formulations for screens with $\beta \sim 0.6$, which were derived and verified in Ref. 15, are

$$\alpha = 0.66 + 0.31/(1 + K_\theta)^{0.5} \tag{7}$$

instead of the generally accepted form,

$$\alpha = 1.1/(1 + K)^{0.5} \tag{8}$$

and for α_θ

$$\alpha_\theta = \frac{1}{\theta}\tan^{-1}\left[\tan\theta - \frac{\theta}{2}\sec^2\theta\left(\frac{F_\theta}{\theta}\right)F\right] \tag{9}$$

where

$$\frac{F_\theta}{\theta} = \left[0.68 - \left(\frac{0.62}{(1 + K_\theta)^{0.5}}\right)\right]$$

and

$$F = (1.0 + 1.5\theta)$$

Thus, for the limiting case of $\theta = 0$, Eq. (7) is of the same form as Eq. (8), and for $\theta > 0$, α_θ can be evaluated using Eq. (9), given θ and K. This semiempirical prediction formula is compared to the measured values of α_θ in Fig. 9. On the whole, agreement to within 10% was obtained for all the screens, implying good collapse of the quantities on which the correlations were based. However, a need for more accurate data is evident in order to test and improve the present models.

Conclusions

Basic differences have been shown to exist between the effects of plastic and metal screens. This is due mainly to the different weaving properties and elastic moduli of the fibers.

Overshoot in mean velocity is attributed to the effects of streamline or screen inclination, and it is greater for plastic screens due to the latter effect. Beyond the boundary layer, metal screens produced more nonuniformities than the plastic ones, and this is correlated with the uniformity of weave. Recovery of the mean flow is complete by about $x = 600$ mm ($\equiv 40\delta_0$), although the overshoot from plastic screens is persistent.

The effect of all the screens on turbulence structure is similar: the existing turbulence is almost completely obliterated and a "new" boundary layer is formed, with increased activity in the inner part of the outer layer. The recovery of the boundary-layer turbulence structure is also almost complete by about $x = 40\delta_0$.

Interesting results have emerged from this investigation for K_θ and α_θ. The results clearly show that an important parameter in determining the trends is the open-area ratio. For screens normally used today in wind tunnels, $\beta \sim 0.6$, and so the relations derived in the present investigation are more applicable.

Acknowledgments

The author is extremely grateful to Professor P. Bradshaw for many helpful suggestions during the course of this study. Also, the helpful comments of Dr. R.V. Westphal and Dr. J. Scheiman on an earlier draft of this paper are acknowledged.

References

[1]Prandtl, L., "The Attainment of a Steady Air Stream in Wind Tunnels," NACA-TM-726, 1933.

[2]Dryden, H.L. and Schubauer, G.B., "Use of Damping Screens for Reduction of Wind Tunnel Turbulence," *Journal of the Aeronautical Sciences*, Vol. 14, 1947, p. 221.

[3]Taylor, G.I. and Batchelor, G.K., "The Effect of a Wire Gauze on a Small Disturbance in a Uniform Stream," *Quarterly Journal of Mechanics and Applied Mathematics*, Vol. 2, 1949, p. 1.

[4]Townsend, A.A., "The Passage of Turbulence Through Wire Gauzes," *Quarterly Journal of Mechanics and Applied Mathematics*, Vol. 4, 1951, p. 308.

[5]Corrsin, S., "Turbulence: Experimental Methods," *Handbuch der Physik*, Vol. 8, Springer-Verlag, Berlin, 1963, p. 523.

[6]Loehrke, R.I. and Nagib, H.M., "Control of Free-Stream Turbulence by Means of Honeycombs: A Balance Between Suppression and Generation," *ASME Journal of Fluids Engineering*, Vol. 98I, 1976, p. 342.

[7]Scheiman, J. and Brooks, J.D., "Comparison of Experimental and Theoretical Turbulence Reduction from Screens, Honeycomb, and Honeycomb-Screen Combinations," *Journal of Aircraft*, Vol. 18, 1981, p. 638.

[8]Tan-Atichat, J., Nagib, H.M., and Loehrke, R.I., "Interaction of Free-Stream Turbulence with Screens and Grids: A Balance Between Turbulence Scales," *Journal of Fluid Mechanics*, Vol. 114, 1982, p. 501.

[9]Bushnell, D.M., "Body-Turbulence Interaction," AIAA Paper 84-1527, 1984.

[10]Collar, A.R., "The Effect of a Gauze on the Velocity Distribution in a Uniform Duct," Aeronautical Research Council R&M 1867, 1939.

[11]Annand, W.J.D., "The Resistance to Airflow of Wire Gauzes," *Journal of the Royal Aeronautical Society*, Vol. 57, 1953, p. 141.

[12]Wieghardt, K.E.G., "On the Resistance of Screens," *Aeronautical Quarterly*, Vol. 4, 1953, p. 186.

[13]Davis, G. de V., "The Flow of Air Through Wire Screens," *Hydraulics and Fluid Mechanics*, edited by R. Silvester, Pergamon Press, London, 1964, pp. 191-212.

[14]Mehta, R.D., "Turbulent Flow Through Screens," AIAA Paper 84-0538, 1984.

[15]Mehta, R.D., "Aspects of the Design and Performance of Blower Tunnel Components," Ph.D. Thesis, Aeronautics Department, Imperial College, London University, UK, 1978 (available on microfiche from Imperial College).

[16]Schubauer, G.B., Spangenberg, W.G., and Klebanoff, P.S., "Aerodynamic Characteristics of Damping Screens," NACA-TN-2001, 1950.

[17]Gibbings, J.C., "The Pyramid Gauze Diffuser," *Ingeneur-Archiv*, Vol. 42, 1973, p. 225.

[18]Carrothers, P.J.G. and Baines, W.D., "Forces on Screens Inclined to a Fluid Flow," *ASME Journal of Fluids Engineering*, Vol. 97I, 1965, p. 116.

[19]Reynolds, A.J., "Flow Deflection by Gauze Screens," *Journal of Mechanical Engineering Science*, Vol. 11, 1969, p. 290.

[20]Simmons, L.F.G. and Cowdrey, C.F., "Measurements of the Aerodynamic Forces Acting on Porous Screens," Aeronautical Research Council R&M 2276, 1945.

[21]Laws, E.M. and Livesey, J.L., "Flow Through Screens," *Annual Review of Fluid Mechanics*, Vol. 10, 1978, p. 247.

[22]Mehta, R.D., "Aerodynamic Design of Blower Tunnels with Wide-Angle Diffusers," *Progress in Aerospace Science*, Vol. 18, No. 1, 1977, pp. 59-120.

[23]Mehta, R.D. and Bradshaw, P., "Design Rules for Small Low Speed Wind Tunnels," *Aeronautical Journal*, Vol. 83, No. 827, 1979, pp. 443, 449.

[24]Bradshaw, P., "The Effect of Wind Tunnel Screens on Nominally Two-Dimensional Boundary Layers," *Journal of Fluid Mechanics*, Vol. 22, 1965, p. 679.

[25]Baines, W.D. and Peterson, E.G., "An Investigation of Flow Through Screens," *Transactions of the ASME*, Vol. 73, 1951, p. 467.

[26]Morgan, P.G., "The Stability of Flow Through Porous Screens," *Journal of the Royal Aeronautical Society*, Vol. 64, 1960, p. 359.

[27]Owen, P.R. and Zienkiewicz, H.K., "The Production of Uniform Shear Flow in a Wind Tunnel," *Journal of Fluid Mechanics*, Vol. 2, 1957, p. 521.

[28]Corner, J.C., "The Effect of a Gauze on a Turbulent Boundary Layer," M.Sc. Thesis, Imperial College, London University, UK, 1971.

[29]Lau, Y.L. and Baines, W.D., "Flow of Stratified Fluid Through Curved Screens," *Journal of Fluid Mechanics*, Vol. 33, 1968, p. 721.